Surface Topography and Composition of Deuterated Polystyrene−Poly(bromostyrene) Blends

Stanley Affrossman,*,† Guido Henn,‡ Scott A. O'Neill,† Richard A. Pethrick,† and Manfred Stamm‡

Department of Pure and Applied Chemistry, University of Strathclyde, Thomas Graham Building, Cathedral Street, Glasgow G1 1XL, UK, and Max-Planck Institut für Polymerforschung, Postfach 3148, 55021 Mainz, Germany

Received November 14, 1995[⊗]

ABSTRACT: Surface structure, obtained from atomic force microscopy and X-ray reflectivity, and surface chemical analysis data, obtained from X-ray photoelectron and static secondary ion mass spectroscopy, are reported for blends of poly(*p*-bromostyrene) with poly(deuteriostyrene). When high speeds are used in the spin-coating process, the atomic force microscopy measurements reveal that the surface structure consists of islands, the distribution and number changing with the poly(bromostyrene) content. A ribbon structure is observed at just above 50% (w/w) poly(bromostyrene) in the mixture. These ribbons merge to form more continuous structures, leaving voids at higher concentrations. X-ray reflectivity data from the films were consistent with the topographical features observed with the AFM. At low spinning speeds, continuous films with little or no topographical structure are formed. The islands observed at high spinning speeds are predominately poly(bromostyrene) and reflect the importance of thermodynamic and kinetic driving forces in their formation.

INTRODUCTION

Spin coating is widely used in the production of thin films in the semi conductor industry.[1,2] The film formation process involves the interplay of a number of time-dependent processes:[3,4] solvent evaporation, gelation, elongational flow under a shear field, wetting, vitrification, solvent diffusion, etc. Because of its practical importance the process of thin-film formation has been studied by a variety of techniques[1−4] and most recently by scanning surface microscopies.[5,6] Studies on dilute solutions have indicated that below a critical concentration, C^*, corresponding to the overlap of polymer coils a homogeneous film is not formed and Voronoi tessellation network structures are produced, a typical value for C^* for a polymer with molecular weight 10^5 being 0.05% (w/v). The network is constructed from particles with sizes ranging from those of a single polymer coil to larger polymer aggregates.[5] At higher concentrations, pinhole-free, smooth films are produced under certain conditions. The precise concentration at which a continuous film is produced depends on the molecular weight, polydispersity, and polymer−solvent interaction parameters. Thin continuous films of ∼100 nm thickness may break up on heating for several hours close to their glass transition temperature, T_g, to form a tessellation pattern in which small aggregates of polymer beads appear to be distributed across the silicon wafer surface. The concentration for continuous film formation is therefore a delicate balance between achieving coil overlap and the complex interplay of forces at the air−polymer and solution−substrate interfaces.

Polymer blends exhibit even more complex behavior on spin casting, related to the possibility of phase separation occurring during film formation. Thin films of polystyrene (PS) with poly(vinyl methyl ether) (PVME) exhibit structures which are attributed to demixing during film formation.[6] Interaction of the polymers with the substrate plays a important part in formation of topographical features, with interface-induced spinodal decomposition having a dominant effect for very thin films, $\sim<0.1\ \mu$m.[7] The spinodal point has been observed to decrease below room temperature with decreasing film thickness for films of less than ∼30 nm.[8] The interference of the spinodal waves originating from the two interfaces has been noted, and offset of the spinodal waves originating from two interfaces was confirmed when the film thickness was smaller than 500 nm. Oscillatory structure in such systems has been investigated[9] and found to be a complex interplay between phase separation and wetting of the substrate.[10−15] Various attempts have been made using polymeric thin films to study phase separation in reduced dimensionality. For the diffusion-limited stage of spinodal decomposition, a power law growth of the characteristic domain size is expected, with an exponent $^1/_3$ independent of the dimensionality of the domains,[16] which appears to be consistent with experimental observation.[14,15,17]

This paper explores the relationship between topographical structure and variation in composition of spin cast films of blends of poly(styrene-d_8) (PdS) with poly(*p*-bromostyrene) [P(Br_xS)]. The properties of the PdS/P(Br_xS) system change with the degree of bromination, *x*, enabling mixtures with various degrees of miscibility to be generated, and a number of studies of segregation and polymer diffusion have been reported.[18−20] The degree of bromination controls the miscibility of these polymer mixtures; however, the structures observed are influenced by the nature of the substrate used.[11]

Surface energy is an important factor in the segregation of blend components, and the component with the lower surface energy is generally enriched at the surface. Even for isotopic mixtures of deuterated and protonated polystyrene, segregation of the lower energy component has been shown by a range of techniques including neutron reflection[21,22] and secondary ion mass spectroscopy (SIMS).[23] In this study, atomic force microscopy (AFM) and X-ray reflectivity combined with X-ray photoelectron spectroscopy (XPS) and static SIMS are used to characterize the surface topography and composition of a series of blends.

† University of Strathclyde.
‡ Max-Planck Institut für Polymerforschung.
[⊗] Abstract published in *Advance ACS Abstracts,* June 1, 1996.

S0024-9297(95)01691-3 CCC: $12.00

Table 1. Variation of the Polymer Film Features with Composition for PdS/P($Br_{1.0}$S) Blends

Figure 1 panel	compstn of polym blend (% (w/w) P($Br_{1.0}$S))	film thickness (nm)	features	typical island ht or hole depth (nm)	typical diam (nm)
b	10	42 ± 4	islands	12 ± 3	139 ± 23
c	30	39 ± 6	islands	12 ± 1	197 ± 15
d	50	40 ± 3	islands	15 ± 1	317 ± 64
e	60	39 ± 3	ribbons	13 ± 1	
f	70	39 ± 4	holes	15 ± 1	656 ± 125
g	75	40 ± 3	holes	12 ± 2	380 ± 88
h	90	39 ± 4	holes	11 ± 1	188 ± 49

EXPERIMENTAL SECTION

Materials. The deuterated polystyrene (PdS) was produced by anionic initiation and had a number-average molecular weight of 1.57×10^5 obtained from GPC. Poly(bromostyrenes) of different degrees of bromination were obtained by a bromination reaction of anionically prepared polystyrene. The degree of bromination was obtained from chemical analysis. The initial polystyrene had a molecular weight of 1.45×10^5, and the polydispersities of the polymers were ∼1.1.

P(Br_xS) is a statistical copolymer of styrene and *p*-bromostyrene, where *x* denotes the degree of bromination (mol %), and in this study we mostly use P($Br_{1.0}$S), where all the para positions of the ring are brominated.

The films were spun at 4000 rpm using a 1.0% (w/v) solution of the polymer blend in toluene onto silicon wafers, with the native oxide retained, to give film thicknesses indicated in Table 1. The concentration used is in sufficient excess of the critical value C^* (0.05% w/v) to assume that uniform films should be formed without pinholes and the tessellation mechanism encountered at lower concentrations should be inoperative. Film thickness was determined with a Sloan Dektak 11a profilometer.

Atomic Force Microscopy. Micrographs of the blend film were recorded with a Burleigh ARIS-3300 Personal AFM. A standard Burleigh AFM probe was used for the measurements. The cantilever, with a silicon pyramidal tip, had a spring constant of ∼0.05 N m^{-1}. Surfaces were imaged at a constant force, typically 8.4 nN.

X-ray Reflectivity. X-ray experiments were performed with a reflectometer with an 18 kW rotating anode generator using Cu Kα radiation.[24] Model fits were calculated using a matrix formalism.[25,26] Interfaces are described by error functions.

X-ray Photoelectron Spectroscopy (XPS) and Static Secondary Ion Mass Spectroscopy (Static SIMS). SIMS analyses were performed using a Vacuum Science Workshop ion gun, operating with a 3 keV argon ion beam at a current of 2×10^{-10} A measured at the gun exit, irradiating an area of ∼5 mm^2. Spectra were obtained with a Vacuum Generators 12-12 quadrupole, fitted with an Einzel lens energy filter. No sample charge compensation was necessary.

X-ray photoelectron spectroscopy data were obtained with a Vacuum Science Workshop X-ray anode, using aluminum or magnesium Kα radiation, and a 100 mm hemispherical analyzer. XPS signals were corrected with Wagner's sensitivity factors, adjusted for our instrument, to give element concentrations.[27]

RESULTS

Atomic Force Microscopy. Initial experiments with blends of PdS and P(Br_xS), with degree of bromination (*x*) varying over the range $x = 0.04-1.0$, showed the presence of distinct surface structures which varied with bromine content. P($Br_{1.0}$S) mixtures proved to give the most striking results and several blend compositions with PdS were investigated, forming the core of the material reported here. At that bromination the blends are known to be incompatible in the bulk.[20] A blend of poly($Br_{1.0}$-styrene) with poly(styrene-h_8) displayed surface features similar to those observed with the deuterated analogues, the slight differences in thermodynamic properties of the deuterated and hydrogenous polymers being outweighed by the effect of the halogen component. The PdS homopolymer films were fairly featureless, Figure 1a, whereas P($Br_{1.0}$S) shows occasional small protrusions. Blending these polymers resulted in very marked topographical features, which changed progressively as the concentration of P($Br_{1.0}$S) increased, Figure 1b−h. At low P($Br_{1.0}$S) concentrations, circular features of height ∼13 nm and width of typically 140 nm are seen, which increase in width with increasing P($Br_{1.0}$S) content. These structures will be referred to as islands. At 60% P($Br_{1.0}$S), a ribbonlike structure is formed, which on further increase in concentration becomes a sheet with holes.

The observed behavior can be described by a model in which it is assumed that the islands are dominantly P($Br_{1.0}$S) and these grow, merge, and eventually completely cover the surface. The model is shown schematically in the following diagram:

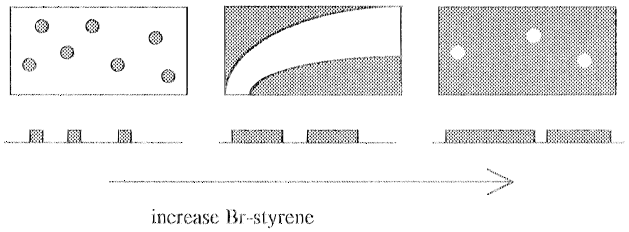

The dark areas indicate regions enriched in P($Br_{1.0}$S) and we will assume, as a first approximation, that they are islands of pure P($Br_{1.0}$S) and the valleys are pure PdS.

The total area occupied by the islands/holes can be obtained from the AFM image and was determined manually. At low Br concentrations the island area was measured, and at high concentrations the area of the holes was subtracted from the total area. The calculated values are referred to as the relative surface coverage and Figure 2 shows the good linear relationship between the relative surface coverage and the bulk P($Br_{1.0}$S) concentration.

The difference in height of the islands and the valleys is only ∼13 nm, which raises the question of the effect of the AFM tip on these observations. Is the "height" difference a result of variation in penetration depths of the tip into patches on the surface and not a real measure of the surface structure? Several runs were carried out with various reference volt settings, corresponding to various tip forces (8−30 nN). The images were all similar and the average heights were within experimental error, providing evidence that the topographical effects are real.

The height of the islands could be altered by changing the spinning speed. Lowering the speed from 4000 to 2000 rpm produced a thicker film and caused the islands to increase in height; e.g., for a 30% P($Br_{1.0}$S) blend the average height was ∼24 nm. Spinning speeds less than 4000 rpm tended to give uneven films with a mixture

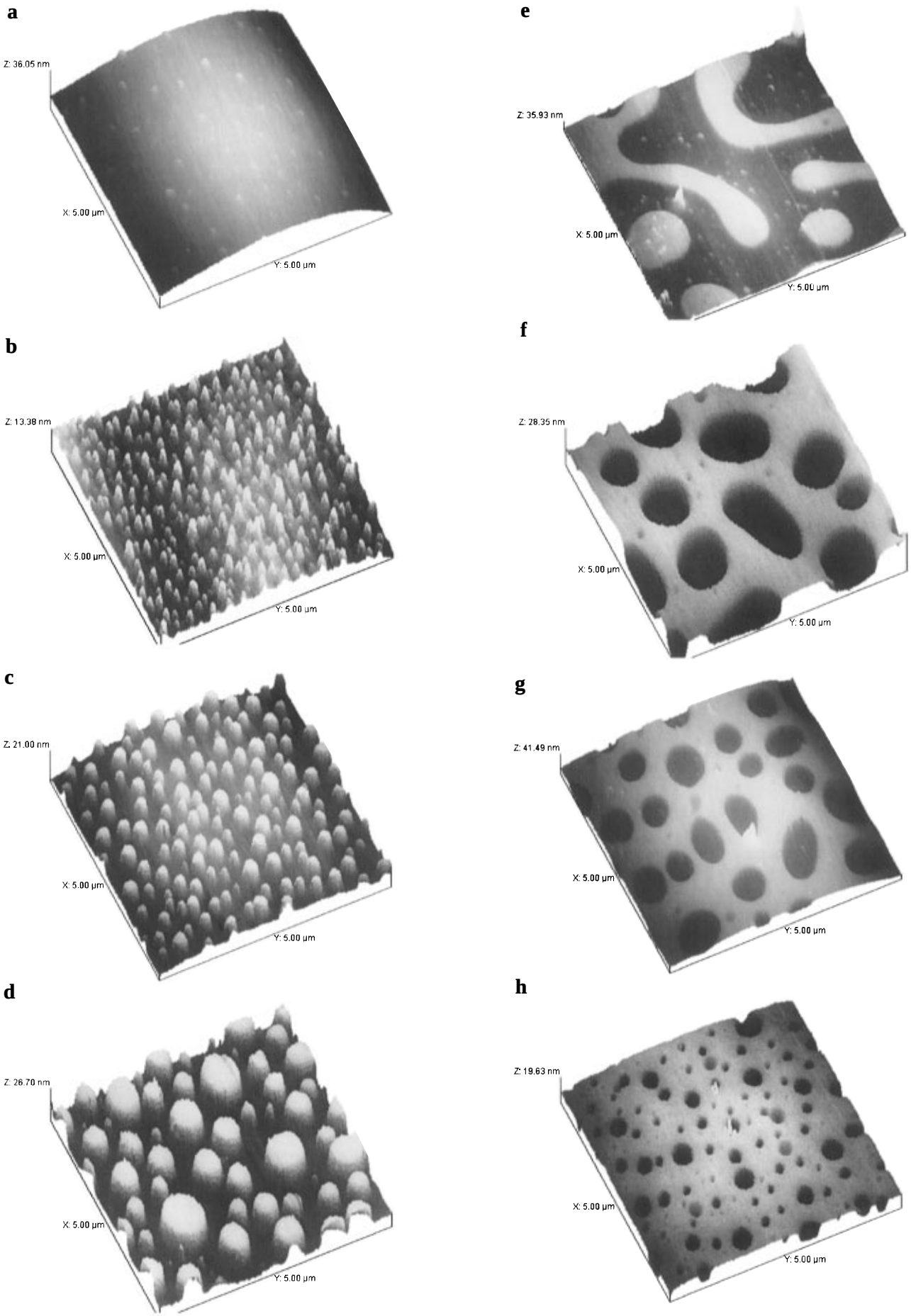

Figure 1. AFM images of poly(styrene-d_8)/poly($Br_{1.0}S$) blends. P($Br_{1.0}S$) (%, w/w): (a) 100, (b) 10, (c) 30, (d) 50, (e) 60, (f) 70, (g) 75, and (h) 90.

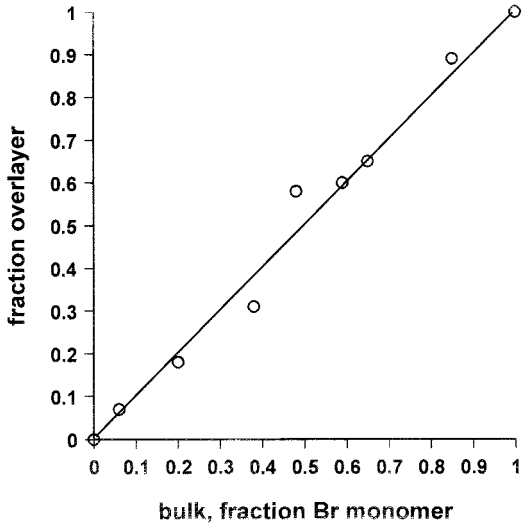

Figure 2. Overlayer coverage from AFM image versus bulk P($Br_{1.0}$S) monomer fraction.

of feature types, and at less than 1000 rpm no marked features were obtained.

X-ray Reflectivity. Two blends were selected for X-ray reflectivity analysis, 30:70 and 70:30% P($Br_{1.0}$S)/PdS. The X-ray reflection curve obtained from the 30:70 P($Br_{1.0}$S)/PdS blend is presented in Figure 3a. The experimental data can be fitted with a two-layer electron density profile, given in the inset of the figure, indicative of a homogeneous film (28.6 nm thick) with an increased surface roughness. The surface roughness is modeled by an 8 nm thick second layer on top of the homogeneous film, with an electron density ~80% less than film below. Since X-ray reflection laterally averages both air and polymer at the surface, the 8 nm thick layer simulating the film's roughness can be interpreted as small islands on top of a homogeneous film.

The X-ray reflection curve obtained from the 70:30 P($Br_{1.0}$S)/PdS blend is presented in Figure 3b. The experimental data are fitted to a two-layer electron density profile, shown in the inset. The electron density of the top layer (11.6 nm thick) is 27% less than the electron density of the bottom layer (20.8 nm thick). Again, the data are consistent with an overlayer of islands on top of a homogeneous film.

The X-ray reflectivity data confirm the topography observed with the AFM, and the total (island + sublayer) thicknesses of ~32−37 nm are comparable with the profilometer value of ~39 nm (Table 1). The height of the islands measured by AFM is ~13 nm, which agrees well with the X-ray reflectivity value of 12 nm for the 70:30 P($Br_{1.0}$S)/PdS blend.

The X-ray reflectivity measurement for the height of the islands of the 30:70 P($Br_{1.0}$S)/PdS blend, ~8 nm, is apparently in poorer agreement with the AFM data (~13 nm). However, from inspection of the AFM image it is seen that there is a distribution of island heights, and the statistics of fitting the X-ray data, Figure 3a, are not as good as for the 70:30 P($Br_{1.0}$S)/PdS blend. Also, separate samples were used for AFM and X-ray reflectivity.

X-Ray Photoelectron Spectroscopy of Pure Compounds and Blends: Pure Components. The sample depth of XPS is ~5 nm and the area probed is ~10 mm^2. The data relate, therefore, to the surface composition averaged over many features seen by the AFM. As a check of the quantification of the XPS experiment, spectra were obtained for a series of P(Br_xS), $x = 0.04-1$, homopolymers. The bromine contents measured, Figure 4, show a linear correlation between the XPS and bulk Br values and indicate that in the pure materials no anomalous features are associated with the surfaces formed. XPS gave a Br:C ratio of 0.117, which is close to the theoretical value of 0.125, for an extent of bromination (x) of 1.0. Substitution of bromine into the

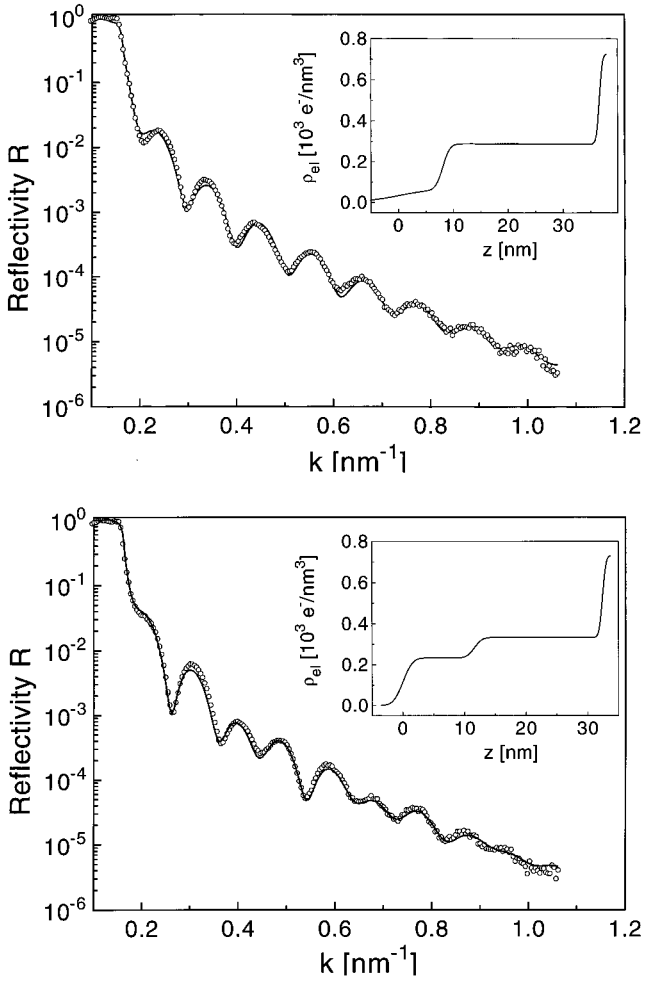

Figure 3. (a, top) X-ray reflectivity data for a 30:70 (w/w) % P($Br_{1.0}$S)/PdS blend: (b, bottom) X-ray reflectivity data for a 70:30 (w/w) % P($Br_{1.0}$S)/PdS blend. Lines are fits to experimental data. The insets give the electron density profile perpendicular to the surface; $z = 0$ at the air polymer interface; k is the momentum transfer.

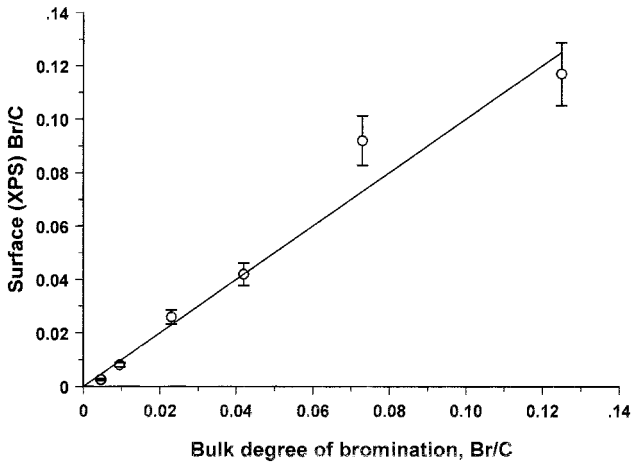

Figure 4. Fraction of bromostyrene at the surface from XPS versus bromine content, x, in poly(Br_x-S) homopolymers. Solid line corresponds to theoretical Br/C ratio for given bulk value.

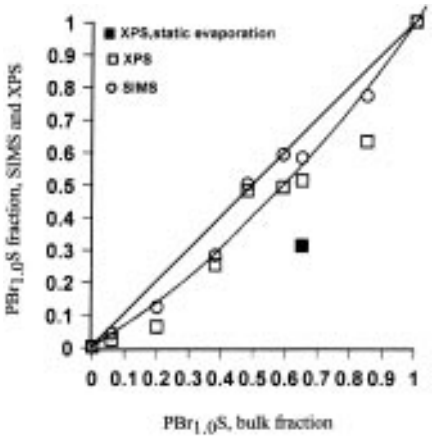

Figure 5. Fraction of bromostyrene at the film surface from XPS or SIMS versus bulk bromine content of blends. Straight line corresponds to 1:1 relationship.

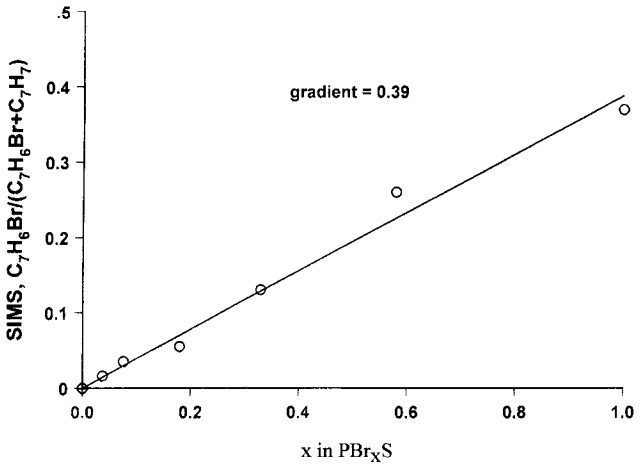

Figure 6. Fraction of bromostyrene at the surface from SIMS versus bromine content, x, in P(Br_xS) homopolymers.

aromatic ring should result in a single bromine atom per styrene monomer, and the XPS data showed that it must also occur statistically along the chain, as local concentrations of brominated material will have a lower surface energy and may be expected to segregate to the surface. The measured Br:C ratio for P($Br_{1.0}$S) also showed that surface impurities cannot be more than a few percent for that polymer.

Blend Composition. The fraction of P($Br_{1.0}$S) at the surface, measured by the bromine concentration determined from XPS, versus the bulk solution composition for the mixtures of blends of P($Br_{1.0}$S) with PdS cast at 4000 rpm is plotted in Figure 5, which shows an increase in P($Br_{1.0}$S) at the surface with increase in bulk P($Br_{1.0}$S). The surface, though, has a relative deficiency in the bromo polymer. In previous studies[20] segregation of PdS to the surface was also observed, but only after annealing, so the observed difference might be due to the extreme surface sensitivity of XPS. A film prepared by allowing solvent to evaporate without spinning gave a lower surface P($Br_{1.0}$S) content than the corresponding spin-cast sample, Figure 5, showing that with the faster solvent evaporation of the spin-cast conditions the surface segregation of PdS is reduced. This may indicate that the equilibrium distribution is in favor of a strong PdS segregation to the surface.

In Figure 4, the deviations from the predicted composition curve obtained from XPS data for the series of brominated homopolymers were mainly small. The scatter of values in the data for the blends, Figure 5, reflects the variability in composition resulting from the surface structure of the film, which is critically dependent on the procedure used in their generation.

Static Secondary Ion Mass Spectroscopy of Pure Compounds and Blends: Pure Components. The static SIMS spectrum for the PdS was in agreement with published data[28] and showed no significant impurities. The principal ion detected was, as expected, $C_7D_7^+$, with a negligible contribution at 91 Da, $C_7H_7^+$.[29] The static SIMS spectrum for P($Br_{1.0}$S) should have a corresponding principal signal $C_7H_6Br^+$, with no $C_7H_7^+$ if $x = 1$. A significant $C_7H_7^+$ signal was however detected. There are three possible causes for this result; first, impurities are present which have a styrene-like structure; second, the Br/monomer stoichiometry is not 1.0 in these polymers; or third, rearrangement occurs of the structure from $-(C_8H_7Br)-$ to $C_7H_7^+$ during the SIMS process.

The XPS data, Figure 4, indicate that the impurity concentration cannot be more than a few percent, but even at this level surface-active impurities may migrate to the surface and be very evident in SIMS. The linear correlation in Figure 4 also suggests that the bromine substitution reaction is well behaved, with one bromine per monomer unit, but again, a small amount of unsubstituted chain could be present and may segregate to the surface. The third mechanism, $-(C_8H_7Br)-$ transformation to $C_7H_7^+$, remains a possibility because of the extensive rearrangements that take place when the energy of the incident ion is absorbed by the polymer chain.[30]

The relative amount of brominated material at the surface is obtained from the static SIMS signals for the characteristic fragments from the monomer units, i.e., $[C_7H_6{}^{79}Br^+ + C_7H_6{}^{81}Br^+]/[C_7H_6{}^{79}Br^+ + C_7H_6{}^{81}Br^+ + C_7H_7^+]$, which is plotted, assuming all fragment sensitivities are equal, against the bulk Br content for the series of substituted pure homopolymers in Figure 6. An excellent linear correlation is obtained, though with a gradient of 0.39 rather than 1.0. Impurities would be expected to vary with the polymer sample. Thus, the results for the bromo homopolymers are consistent with the 91 Da signal arising from the fragmentation of the bromo monomer, and the SIMS data may be corrected to give the bromo monomer content by dividing the relative intensity from the bromo fragments by 0.39.

Blend Compositions. The fraction P($Br_{1.0}$S) determined by SIMS versus the bulk composition is shown in figure 5. The data lie close to, but generally below, the 1:1 line and, together with the XPS results, suggest a slight deficiency of P($Br_{1.0}$S) at the surface. The SIMS and XPS surface concentrations do not quite match, which would normally indicate a concentration gradient within the top 4 nm, with the P($Br_{1.0}$S) greater at the outermost layer. However, the data here are not sufficiently accurate to rule out small systematic errors and will therefore be taken to mean that XPS and SIMS both show a correlation of the P($Br_{1.0}$S) at the surface with the bulk composition, with the surface having overall a slightly reduced concentration.

DISCUSSION

Model for the Overlayer. The consensus, in particular from neutron reflectrometry experiments,[20] is that PdS segregates to the surface of poly(styrene-d_8/poly(bromostyrene) blends. The XPS results show an excess of PdS for the series of blends examined, and the deviation from the bulk value is seen to depend on the conditions used for film formation, with spin speeds of

4000 rpm giving a small but marked effect. Neglecting the disparity in surface and bulk concentrations for the moment, the good correlation between the total overlayer area and the bulk P($Br_{1.0}$S) concentration of the casting solution suggests initially a simple model of random nucleation of P($Br_{1.0}$S) to form islands in a sea of PdS. It is a moot point whether the PdS and P($Br_{1.0}$S) deposit simultaneously, but in any event the film is formed from a three-component system, i.e., includes solvent, and because of rapid removal of the latter ends up as a two-phase film frozen in a nonequilibrium configuration.

In the most simplistic case, the overlayer area/bulk concentration relationship suggests that the volume of the overlayer of P($Br_{1.0}$S) should correspond to the bulk concentration. The packing of monomer units in the very thin film is unknown, but assuming that the monomer molar volumes relate to the measured densities of P($Br_{1.0}$S) and PS, 1.4052 and 1.0482 g cm^{-3}, respectively, leads to a relative monomer molar volume of 1.30:1. The bromo polymer is prepared from PhS with an equivalent degree of polymerization to the PdS; thus the relative polymer volumes are also 1.30:1. If the islands of P($Br_{1.0}$S) are anchored at the wafer substrate then, because of the observed overlayer area/bulk monomer concentration relationship, the ratio of the height of the islands to that of the valleys, measured from the wafer, should be 1.30:1. The AFM value is 1.32 ± 0.06:1.

The data therefore indicate that the film is formed via a random nucleation mechanism with separation of the phases, and the P($Br_{1.0}$S) nuclei grow laterally to produce islands of approximately uniform height, 40 nm, over the full concentration range of P($Br_{1.0}$S). A major constraint on the vertical growth will be the small amount of solution retained as a film during the spinning process. Within this liquid film, adhesion of P($Br_{1.0}$S) to the substrate would cause the islands to spread out rather than grow vertically, though this would be opposed by chain entanglements. In a study of a similar blend, though with thicker films which were annealed, Krausch et al.[31] concluded that there was no preferential wetting of the oxide surface by either component, i.e., no bilayer at the silicon interface, which is accord with the model proposed above.

Considering now the XPS data, the phase-separated model has the consequence that the XPS signal from a component will depend on the exposed area of the phase. It has been seen that the topographical relationship of P($Br_{1.0}$S) and PdS can be understood in terms of the relative molar volumes. The XPS data are in terms of the monomer concentrations; therefore, it is necessary to derive the relative monomer molar areas. Using the above densities, the relative molar areas are PdS: P($Br_{1.0}$S) = 0.838. Therefore, for a given P($Br_{1.0}$S) fraction area, the P($Br_{1.0}$S) fraction monomer is area P($Br_{1.0}$S)/[area P($Br_{1.0}$S) + area PdS/0.838]; e.g., for a bulk concentration of P($Br_{1.0}$S) = 0.5, and therefore area fraction of 0.5, the monomer fraction is 0.46. The XPS measurement for P($Br_{1.0}$S) at this bulk concentration, figure 5, is ∼0.40, which suggests that the P($Br_{1.0}$S) is not pure, having entrapped PdS during the rapid evaporation of solvent, and the scatter of data reflects the critical nature of the process. Entrapped PdS may feasibly segregate to the surface of the P($Br_{1.0}$S).

Lower spinning speed gives a longer time for binodal/spinodal decomposition to take place at the air−polymer solution and solution−substrate interfaces, and a thicker surface layer structure is obtained. At less than 1000 rpm, the slower speeds will allow time for particle coalescence to form a continuous film, which implies that the T_g must be suppressed by the slower solvent evaporation rates. The segregation of PdS to the surface is also facilitated, leading to a large surface excess. Above this spinning speed, the evaporation rates are sufficiently high to freeze in the initial kinetics of nucleation, raise the T_g rapidly, and give the structures observed.

CONCLUSIONS

Marked topographic features in a range of sizes can be consistently obtained on thin films of blends of P($Br_{1.0}$S) and PdS by control of the solution concentration and film deposition conditions. The raised features observed by AFM are dominated by aggregations of molecules of P($Br_{1.0}$S) which grow with increase in bulk P($Br_{1.0}$S) concentration. Lowering the spinning speed allows thickening of the surface layer to occur with the formation of a continuous smooth layer. Whether or not the surface topography is formed depends critically on the physical properties of the polymers, the process whereby they segregate in the bipolymer−solvent system, and the dynamics of solvent removal.

Acknowledgment. We are grateful to Th. Wagner for help with sample preparation and characterization. We also appreciate financial support from EPSRC (studentship), BMBF (Project F13MPG), and the EU (Framework Contracts CT930351 and CT930370).

References and Notes

(1) Thompson, L. F.; Grant, W. C.; Bowden, M. J. *Introduction to Lithography*, 2nd ed.; American Chemical Society: Washington, DC, 1994; p 308.
(2) Thompson, L. F.; Grant, W. C.; Bowden, M. J. *Introduction to Lithography*; American Chemical Society: Washington, DC, 1983; p 183.
(3) La Vergne, D. B.; Hofer, D. C. *Proc. SPIE* **1985**, *539*, 115.
(4) Bornside, D.; Macosko, C. W.; Scriven, L. E. *J. Imaging Technol.* **1987**, *13*, 122.
(5) Stange, T. G.; Mathew, R.; Evans, D. F.; Hendricksen, W. A. *Langmuir* **1992**, *8*, 920.
(6) Tanaka, K.; Yoon J.-S.; Takahara, A.; Kajiyama, T. *Macromolecules* **1995**, *28*, 934.
(7) Krausch, G.; Dai, C. A.; Kramer, E. J.; Marko, J. F.; Bates, F. S. *Macromolecules* **1993**, *26*, 5566.
(8) Reich, S.; Cohen, Y. *J. Polym Sci., Polym. Phys. Ed.* **1981**, *19*, 1255.
(9) Jones, R. A. L.; Norton, L. J.; Kramer, E. J.; Bates, F. S.; Wiltzius, P. *Phys. Rev. Lett.* **1991**, *66*, 1326.
(10) Wiltzius, P.; Cumming, A. *Phys. Rev. Lett.* **1991**, *66*, 3000.
(11) Bruder, F.; Brenn, R. *Phys. Rev. Lett.* **1992**, *69*, 624.
(12) Tanka, H. *Phys Rev. Lett.* **1993**, *53*, 2770.
(13) Ball, R. C.; Essery, R. H. L. *J. Phys Condens. Matter* **1990**, *2*, 1030.
(14) Puri, S.; Binder, K. *Phys Rev., A* **1992**, *46*, R4478; *Phys Rev., E* **1994**, *49*, 5359.
(15) Marko, J. F. *Phys Rev., E* **1993**, *48*, 2861.
(16) Marqusee, J. A. *J. Chem Phys.* **1984**, *81*, 976.
(17) Brown, G.; Chakrabarti, A. *Phys Rev.* **1992**, *46*, 4829.
(18) Guckenbiehl, B.; Stamm, M.; Springer, T. *Colloids Surf. A* **1994**, *86*, 311.
(19) Bruder, F.; Brenn, R. *Europhys. Lett.* **1993**, *22*, 707.
(20) Guckenbeihl, B.; Stamm, M.; Springer T. *Physica B* **1994**, *198*, 127.
(21) Jones, R. A. L.; Kramer, E. J. *Philos. Mag.* **1990**, *B29*, 129.
(22) Jones, R. A. L.; Norton, L. J.; Kramer, E. J.; Composto, R. J.; Stein, R. S.; Russell, T. P.; Mansour, A.; Karim, A.; Felcher, G. P.; Rafailovich, M. H.; Sokolov, J.; Zhao, X.; Schwarz, S. A. *Europhys. Lett.* **1990**, *12*, 41.
(23) Zhao, X.; Zhao, W.; Schwarz, S. A.; Wilkens, B. J.; Rafailovich, M. H.; Sokolov, J.; Jones, R. A. L.; Kramer, E. J. *Macromolecules* **1991**, *24*, 5991.

(24) Foster, M.; Stamm, M.; Reiter, G.; Hüttenbach, S. *Vacuum* **1990**, *41*, 1441.
(25) Lekner, J. *Theory of Reflection*; Martin Nijhoff: Amsterdam, 1987.
(26) Stamm, M. In *Physics of Polymer Surfaces and Interfaces*; Sanchez, I. C., Ed.; Butterworth-Heinemann: Boston, 1992.
(27) *Practical Surface Analysis;* Briggs, D., Seah, M. P., Eds.; John Wiley: Chichester, U.K., 1990; Vol. 1.
(28) Jones, R. A. L.; Kramer, E. J. *Polymer* **1993**, *34*, 115.
(29) Affrossman, S.; Hartshorne, M.; Jerome, J.; Munro, H. S.; Pethrick, R. A.; Petijean, S.; Rei Vilar, M. *Macromolecules* **1993**, *26*, 5400.
(30) Chilkoti, A.; Castner, D. G.; Ratner, B. D. *Appl. Spectrosc.* **1991**, *45*, 209.
(31) Krausch, G.; Kramer, E. J.; Rafailovich, M. H.; Sokolov, J. *Appl. Phys. Lett.* **1994**, *64*, 2655.

MA9516910